3

Novel Challenges in Crystal Engineering: Polymorphs and New Crystal Forms of Active Pharmaceutical Ingredients

Vânia André and M. Teresa Duarte
Centro de Química Estrutural, Dept. of Chemical and Biological Engineering, Instituto Superior Técnico, Universidade Técnica de Lisboa, Lisbon Portugal

1. Introduction

Crystal engineering and co-crystallization have evolved in recent years and gained a special interest not only in academia but also in the pharmaceutical field as it has been shown that the physical and pharmacokinetic properties of new crystal forms (solvates, salts, molecular salts, co-crystals, polymorphs) are different when compared to pure APIs[1-16]. Actually, producing co-crystals of pharmaceuticals has been reported to change their melting points[3], solubility and dissolution rates[2, 4], moisture uptake[17], physical and chemical stability[18] and *in vivo* exposure[9, 19-21]. The leading idea is that the potentiality of new different forms may open to innovation and new drug discoveries as well as to intellectual property protection via patenting of new forms of "old drugs"[5, 7, 22]. The diversity of forms that crystalline solids may attain is mainly due to non-covalent interactions resulting in different molecular assemblies that imply an energetic interplay between enthalpy and entropy.

Although organic salts are traditionally the preferred crystal form of APIs because of their higher solubility and/or increased degree of crystallinity, the potential number of suitable organic salts is limited to the counterions specified by the Food and Drug Administration (FDA) as generally regarded as safe (GRAS). This limitation stimulates the development of other suitable forms and recently co-crystals have been gaining relevance in studies and some of them have already shown to improve therapeutic utility as well as reducing the side effects even when compared with marketed drugs. Consequently, APIs represent a particular great challenge to crystal engineers, because they are inherently predisposed for self-assembly since their utility is usually the result of the presence of one or more exofunctional supramolecular moieties. However, the crystal packing of APIs is even less predictable than that of other organics due to their multiple avenues for self-assembly. Additionally, APIs are commonly valuable chemical entities and therefore the diversity of the crystal forms of those molecules is of great importance for the variability of properties and potential intellectual property.

Co-crystals are most commonly thought of as structural homogeneous crystalline materials that contain two or more neutral building blocks that are present in definite stoichiometric amounts and are obtained through the establishment of strong hydrogen bonds and other non-covalent interactions such as halogen bonds, π-π and coulombic interactions. However,

if the groups involved in these bonds have the tendency to transfer protons between acids and bases, then the result may be a molecular salt instead of a co-crystal. In principle, this event replaces the X-H···Y interaction by a charge assisted $X^{-}\cdots H\text{-}Y^{+}$ hydrogen bond[22].

The formation of multicomponent crystal forms relies mainly on the hydrogen-bond synthons that are possible to form and their relative robustness. Hence a thorough datamining based on the Cambridge Structural Database (CSD)[23], is required for a successful design of the new crystallines. One notable obstacle in the path of rational co-crystal design is the phenomenon of polymorphism, to which organic molecules are predisposed. Polymorphic co-crystals are also not uncommon and a few systems have already been reported to date[24].

Even though co-crystals are traditionally obtained by solution techniques, often limited by differences in solubility of co-crystal components and/or solvent/solute interactions[25], the best strategies to attain the desired forms consist on a judicious choice of synthetic and crystallization conditions, which also contemplate the environment-friendly techniques of mechanochemistry (neat (NG), liquid-assisted (LAG) and ion- and liquid-assisted grinding (ILAG)) that have demonstrated to be an efficient method in co-crystallization screening and synthesis: solid-state grinding allows the formation of multicomponent forms even with low-solubility components that would be difficult to use with the traditional solution techniques; the addition of catalytic amounts of a liquid to the grinding mixture further improves the efficiency of grinding co-crystallization, as already proven[26-30].

Novel crystallines are usually fully characterized using powder (XRPD) and single crystal (SCXRD) X-ray diffraction techniques, differential scanning calorimetry (DSC), thermogravimetric analysis (TGA), hot-stage microscopy (HSM) and spectroscopic methods, such as Fourier transform infrared (FTIR) and Raman.

A wide range of studies have been performed in the last few years, here we will focus on some of those we have been recently engaged. Several studies with gabapentin, a neuroleptic drug, have been reported[31-34] and a few multicomponent crystal forms with carboxylic acids have been exploited and will be deeply discussed in this chapter. With the antibiotic 4-aminosalicylic acid (4ASA) some new crystal forms were disclosed, solvates, and molecular salt[35], showing a clear tendency of this API to form multicomponent crystallines with lone-pair containing heterocycles, such as dioxane, morpholine and piperazine, disrupting the typical $R_2^2(8)$ homosynthon in 4ASA (Figure 1).

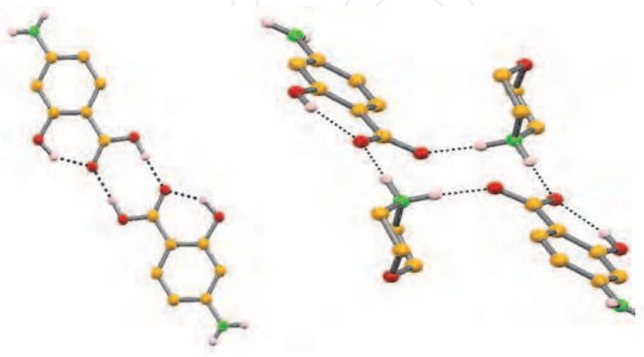

a b

Fig. 1. (a) $R_2^2(8)$ synthon in the 4ASA crystal packing; (b) disrupted $\mathbf{R_2^2(8)}$ synthon in the 4ASA:morpholine molecular salt.[36]

Another example is the widely used paracetamol, which also presents multicomponent crystal forms that were identified and characterized[37-39]. Perindopril erbumine is an antihypertensive drug existent in quite a few polymorphic forms and several hydrates were also disclosed[40-48]. A detailed discussion of some of these compounds will be addressed in this chapter.

But as important as the synthesis of these new compounds is the injunction of their structure-properties relationships. Solubility is a major factor that is known to strongly affect API's performance and therefore its correlation with structural and thermal data is of upmost importance.

API coordination complexes are another related topic that has recently been disclosed as a new pathway for the development of improved crystal forms. In this area, as example, two complexes of 4ASA with silver and one complex coordinating piracetam, a nootropic API, to nickel were prepared and characterized[49].

2. Gabapentin: Polymorphs and multicomponent crystal forms[1,2]

Gabapentin (1-(aminomethyl)cyclohexane acetic acid, GBP) is an analogue of gamma-aminobutyric acid (GABA) and exhibits anticonvulsant properties. It is a neuroleptic drug prescribed for the prevention of seizure, for the treatment of mood disorders, anxiety and tardive diskinesia[50-57], as well as for the treatment of neuropathic pain[58]. More recently, GBP has also been applied in the treatment of limb tremor[59, 60]. This API is highly soluble but has limited and variable bioavailability, probably due to its dependence on a low-capacity aminoacid transporter expressed in a limited region of the upper small intestine. Changes in solid state structure can have marked influence on the physiological absorption characteristics supporting the search for multicomponents crystal forms as means of improving the limited bioavailability of the drug[7, 33, 61, 62].

Gabapentin is known to exist in three anhydrous polymorphic forms[32, 63, 64], which have been the object of many patent applications and issued patents. The nomenclature is not uniform and different publications refer to different forms making use of the same name. One hydrate form, labelled form I, is known[65], while form II is the anhydrous commercial form[66]. The crystal structures of these forms are present in the Cambridge Structural Database (CSD) with the refcodes QIMKOM for form I[67] at -120°C and QIMKIG and QIMKIG01 for form II at -120°C[67] and at RT[58], respectively. Form III as labelled by Braga and co-workers[68], has been described by Pesachovich *et al* [69], and its crystal structure has been reported by Reece and Levendis as form α[70]. A patent by Chen et al[71]. describes a new form of gabapentin, dehydrated A, which is consistent with form β reported by Reece and Levendis[70], labelled form IV by Braga and co-workers[68]. Another crystalline form of gabapentin was described by Lladò *et al*[72], but its powder pattern is very similar to that of

[1] Adapted with permission from On the Track of New Multicomponent Gabapentin Crystal Forms: Synthon Competition and pH Stability,Vânia André, Auguste Fernandes, Pedro Paulo Santos, and M. Teresa Duarte, *Crystal Growth & Design*, 2011, *11* (6), pp 2325–2334,DOI: 10.1021/cg200008z. Copyright (2011) American Chemical Society.

[2] Adapted with permission of the Royal Society of Chemistry (RSC) from Polymorphic gabapentin: thermal behaviour, reactivity and interconversion of forms in solution and solid-state Dario Braga, Fabrizia Grepioni, Lucia Maini, Katia Rubini, Marco Polito, Roberto Brescello, Livius Cotarca, M. Teresa Duarte, Vânia André and M. Fátima M. Piedade *New J. Chem.*, 2008, 32, 1788-1795, DOI: 10.1039/B809662G.

form IV. Kumar *et al*[73] reported a form of gabapentin in an international patent application that is most likely a mixture of forms III and IV (Figure 2).

a b c

Fig. 2. Crystals' morphology of gabapentin polymorphs (a) II, (b) III and (c) IV.

In all characterized forms of gabapentin the molecule crystallizes in its zwitterionic form and hydrogen-bonds consist of charge-assisted N^+-H•••O^- interactions all the supramolecular arrangements relying on chain motifs.

Polymorph II forms double chains that can be seen along b, in which the molecules are oriented so that the substituent groups of the cyclohexane are turned to each other. This orientation of the NH_3^+ and COO^- results in no interactions with neighboring chains along *b* and only one hydrogen bond is used to connect this chain to the parallel chain formed exactly in the same orientation (Figure 3).

In the crystal structure of polymorph III molecules form a 2D sheet along *b*, in which the gabapentin molecules are organized in chains. In the same chain, molecules orient the substituent groups of the cyclohexane ring in the same direction, although the cyclohexane ring is 70.52º alternately rotated. In consecutive chains, the substituent groups are anti-parallel oriented and there are interactions between these two chains (Figure 3).

Several similarities between packing of both forms III and IV of gabapentin can be detected and, indeed, the main difference is that in the latter an intramolecular interaction is established. Form IV also forms chains of gabapentin molecules, in which the cyclohexane structures are rotated alternately rotated by 65.83º. Just as in form III, in each chain the substituent groups are oriented in the same direction and in the chain below have an anti-parallel orientation. The chains are connected in pairs because of the anti-parallel orientation of the substituent groups, which leaves no opportunity to establish hydrogen-bonds with a third chain. However in this form no direct interactions between molecules in the same chain are observed: all of them connect with molecules in the chain above/below and that same molecule that interacts with "initial" molecule will also be connected to the molecule just besides the first one in the other chain. Consecutive parallel chains are formed just ones behind the others, exactly with the same orientation (Figure 3).

Overlapping the structures of the three gabapentin's forms (II, III and IV) it is possible to see that these are conformational polymorphs (Figure 4).

In the three known polymorphs of gabapentin, the carboxylate C-O bond lengths differ by 0.020 Å, 0.017 Å and 0.016 Å in forms II, III and V, respectively. For all these polymorphs, the longer bond involves the O atom that forms two NH···O contacts and the shorter bond is involved only in one NH···O interaction. In all the three structures, the cyclohexane ring adopts an almost perfect chair conformation.

Thermal characterization of the three polymorphs is also reported[68]. In the first DSC heating cycle form II shows an endothermic peak at 158°C (Figure 5) while in the second heating cycle the endothermic peak is at 87°C, thus representing the melting point of gabapentin-lactam[74], confirmed by recrystallization and second heating cycle from the melt on HSM

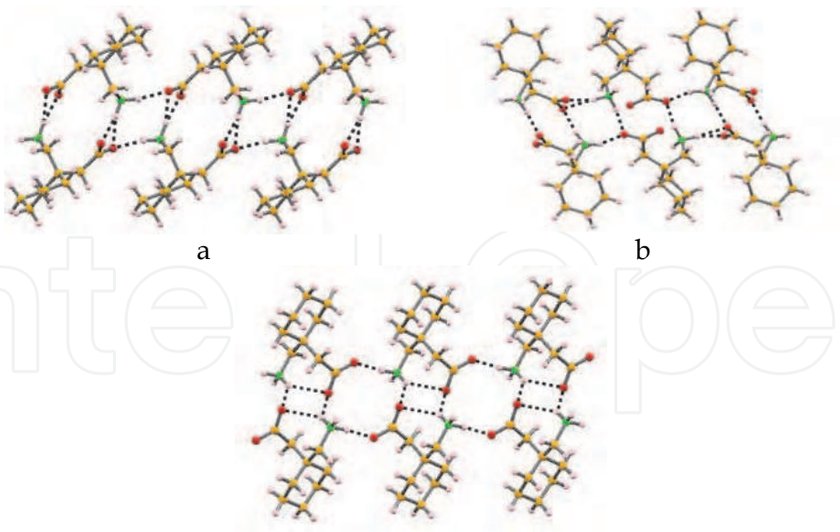

Fig. 3. Supramolecular arrangements of gabapentin forms (a) II, showing the double chains along b, with the substituent groups aligned, (b) III, showing the double chains along b, with the substituent groups rotated and (c) IV showing the double chains assisted by the intramolecular hydrogen bond.

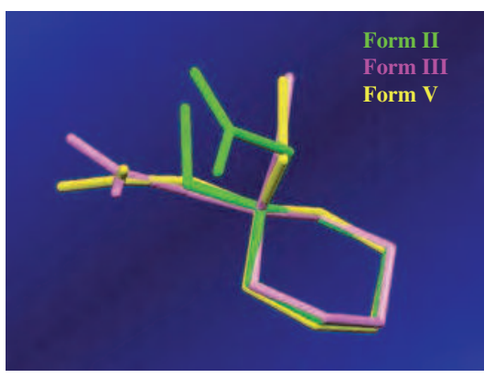

Fig. 4. Gabapentin forms II, III and IV structures overlapped. Hydrogen atoms were omitted for a better visualization.

(Figure 6). The formation of gabapentin-lactam is not surprising, and it is known that gabapentin is unstable in aqueous solutions and undergoes an intramolecular dehydration reaction yielding the lactam[75]; the formation of gabapentin-lactam has also been observed in the solid state[74]. Therefore the endothermic peak observed in the first heating cycle does not correspond to the melting of gabapentin, but covers several events: the cyclization, the release of water and the melting of gabapentin-lactam; these events could not be separated even with a slow scanning rate. Form III shows a similar thermal behaviour, with a broad endothermic peak at 165°C, which is again due to the cyclization process with formation of gabapentin-lactam, water release and melting of gabapentin-lactam[68].

As noted above, the thermodynamic form II undergoes the reaction at a slightly lower temperature than the metastable form III. The different behaviour might be explained by the slightly different pattern of hydrogen bonds in their crystal structures[70].

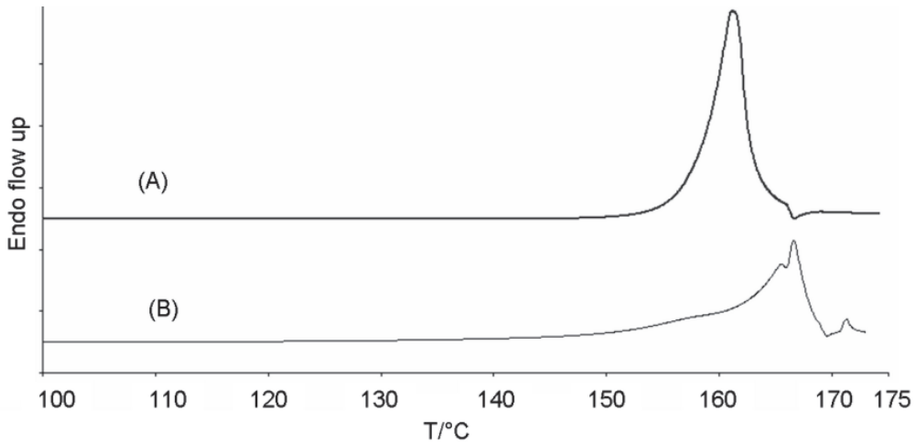

Fig. 5. DSC traces (open pan) of gabapentin Form II (a), with onset temperature = 158.0°C and peak temperature = 161.1°C, and of gabapentin Form III (b), with onset temperature = 165.0°C and peak temperature = 166.6°C[68].

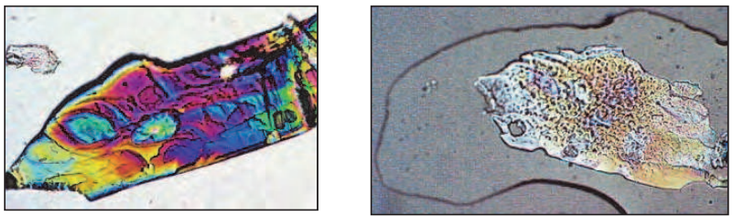

a b

Fig. 6. Hot-stage microscopy of crystalline gabapentin-lactam (a) as obtained in the first DSC heating cycle of gabapentin, showing melting at 89°C (b)[68].

Several attempts to produce pure form IV in reasonable quantity to be used in DSC measurements were not successful; still a HSM experiment on single crystals of form IV isolated within an oil drop was possible. Figure 7 clearly shows the release of water as gas bubbles in the temperature range 152-155°C, immediately followed by melting of the gabapentin-lactam thus formed[68].

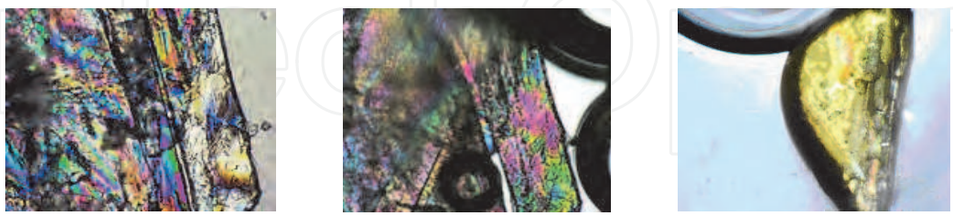

a b c

Fig. 7. Hot-stage microscopy on gabapentin form IV crystals (preserved in Fomblin oil): (a) single crystal at 32°C, (b) evolution of water bubbles at 153°C and (c) complete melting of gabapentin-lactam at 157°C (amplification 100x)[68].

The unique presence in crystals of form IV of an intramolecular N-H···O hydrogen-bond, associated with a smaller number of intermolecular hydrogen bonds with respect to the other two forms, must be responsible for the lower reaction temperature observed[70].

Furthermore, a monohydrate[76-78], two polymorphic chloride hemihydrates[58, 63, 79, 80] an hemisulfate hemihydrate[79, 80] and an heptahydrate under high pressure[81] forms are also known. Coordination complexes of this API with Cu and Zn were isolated and characterized[82]. An extensive pH stability of gabapentin has been disclosed where an ester derivative obtained at low pH was reported[83].

Multicomponent crystal forms (co-crystals and molecular salts) involving GBP with different carboxylic acids were also recently disclosed[1, 32-34].

A search in the Cambridge Structural Database (CSD)[23] (July 2011) has shown that the $R_4^2(8)$ synthon is the most common between cationic amine and carboxylate moieties. The expected synthons to be formed between the API and the coformers should be based on carboxyl···carboxylate and amine···carboxylate interactions. Accordingly to a CSD[23] survey (July 2011), the preferred interactions should be amine···carboxylate followed by the carboxyl···carboxylate.

Therefore, carboxylic acids were chosen as potential coformers of multicomponent crystal forms of gabapentin. Mono and di-carboxylic acids bearing one or more hydroxyl moieties have previously been exploited by Reddy et al[33] revealing an important role of the OH group in the supramolecular arrangements of the new forms. A series of mono-, di- and tricarboxylic acids, without further hydroxyl moieties, were considered by André *et al*[84] to exploit the use of one or more equivalents of carboxylic moieties avoiding the hydroxyl competition.

Five new multicomponent crystal forms of the neuroleptic drug gabapentin with isophthalic acid (pKa1=3.5; pKa2=4.5[85]), phthalic acid (pKa1=3.0; pKa2=5.3[85]), L-glutamine (pKa1=2.1; pKa2=4.3[85]), terephthalic (pKa1=3.5; pKa2=4.5[85]) and trimesic (pKa1=3.1; pKa2=3.9; pKa3=4.7[85]) acids have been reported and are characterized by XRPD. Despite all the crystallization attempts, single crystals suitable for SCXRD were only grown for the compounds with terephthalic (**4**) and trimesic (**5**) acids, which are further characterized by SCXRD, DSC, TGA, HSM and IR. The strong homomeric $R_2^2(8)$ and heteromeric $R_4^2(8)$ synthons observed in the carboxylic acids and gabapentin, respectively, were disrupted and competing synthons based on carboxyl···carboxylate and amine···carboxylate interactions were formed in the new crystallines with trimesic and terephthalic acids[84].

With L-glutamine, a new crystal form **1** characterized by XRPD is obtained by solution techniques. Both solution and LAG experiments with phthalic acid resulted in a mixture of the coformer and a new crystalline **2**. With isophthalic acid, a mixture of a new crystal form **3**, isophthalic acid and gabapentin polymorph III was identified. In this case, the yield of the supramolecular reaction is low and both reagents are also detected, though gabapentin is detected in a different polymorphic form from the starting material. The full conversion into the new form with terephthalic acid, **4**, was only attained by LAG, as terephthalic acid displays solubility problems and showing not only that the formation of this salt is independent of reactional pH but also the advantage of this method when using highly insoluble compounds. The multicomponent crystal form comprising gabapentin and trimesic acid, **5**, was obtained as a single phase both by solution and LAG techniques (Figure 8).

The asymmetric unit of **4** consists on one gabapentin cation and half a terephthalic acid anion residing on an inversion centre. In this structure there is clear evidence of proton transfer between both compounds within the structure and thus this form a molecular salt.

Gabapentin cations are connected to terephthalic anions through three different charge-assisted interactions (Scheme I.a), two of which involve the protonated amine moiety of the

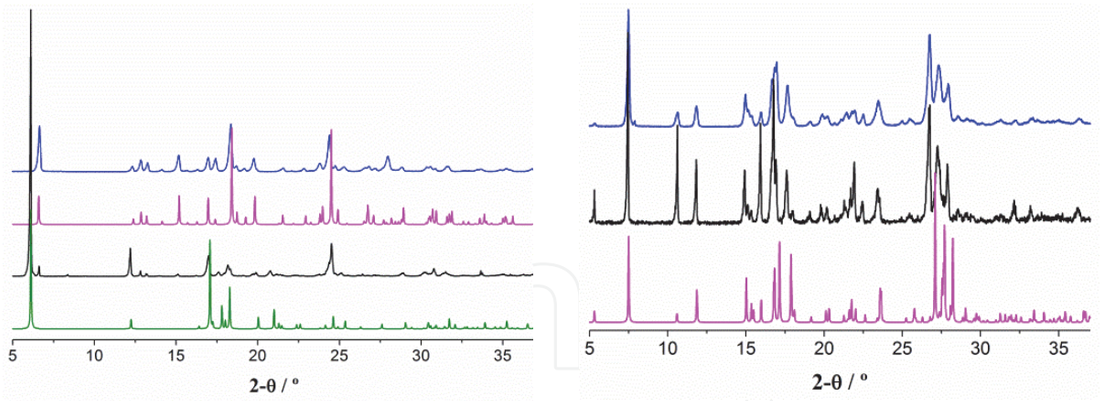

Fig. 8. (a) Experimental XRPD patterns obtained from mechanochemistry (blue); a mixture of gabapentin polymorph III and **4** obtained by solution techniques (black); and gabapentin polymorph III (green); theoretical XRPD patterns obtained from SCXRD data of **4**, at 150K (pink); (b) Experimental XRPD pattern obtained from **5** obtained by LAG (blue) and solution (black) techniques; theoretical powder diffraction pattern obtained from single-crystal data, at 150K (pink).

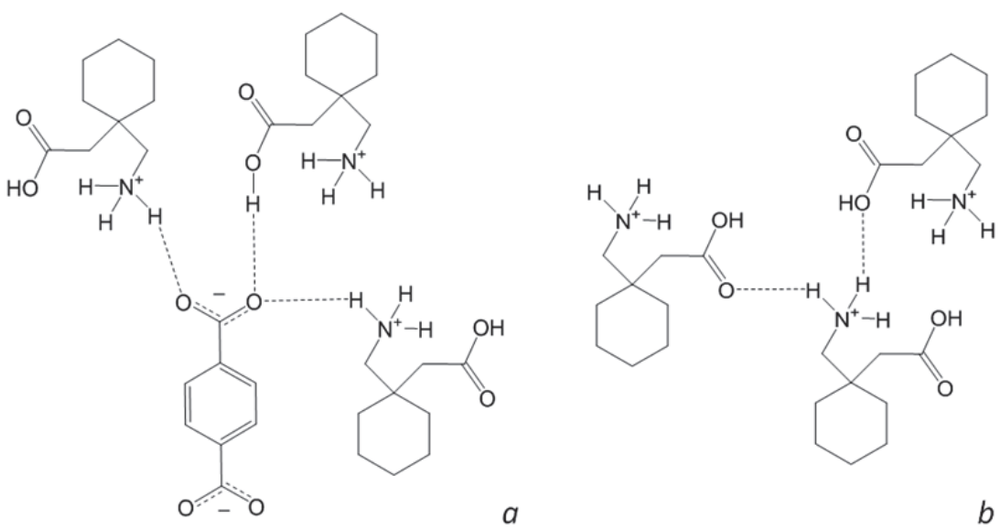

Scheme I. Main hydrogen bond interactions present in molecular salt **4**

API and the carboxylate of the anion, $N^+H_{GBP}\cdots O^-_{TA}$, and a third one concerning the carboxylic group of GBP and again the carboxylate of terephthalic acid, $OH_{GBP}\cdots O^-_{TA}$ (Figure 9.a). The donor group – either the amine and/or the carboxylic moiety – belong to GBP, while the carboxylate groups of terephthalic acid always act as acceptors, with O3 behaving as a bifurcated acceptor.

Gabapentin cations interact among them by the $N^+H_{GBP}\cdots O_{GBP}$ interactions (Scheme I.b), one of them being slightly longer. It is possible to see that these interactions among four gabapentin cations form a tape supported by $R_4^4(12)$ synthons growing along *c* (Figure 9.b).

The interplay of these hydrogen bonds gives rise to terephthalic acid anions acting as spacers between GBP cationic tapes, very clear in a view along the *b* axis (Figure 9.c). Within

the terephthalic acid row, the anionic spacers alternate with a rotation of 27°; it can also be seen that in the gabapentin tape cations are rotated by 39°.
The formation of GBP tapes is a common pattern both in the structure of the three polymorphs of gabapentin and in 4, in the latter the coformer links consecutive tapes. The formation of 4 disrupts the $R_2^2(8)$ synthons typical of the terephthalic acid while increasing the number of hydrogen-bond interactions in which gabapentin is involved when compared with any of the three known polymorphic forms.

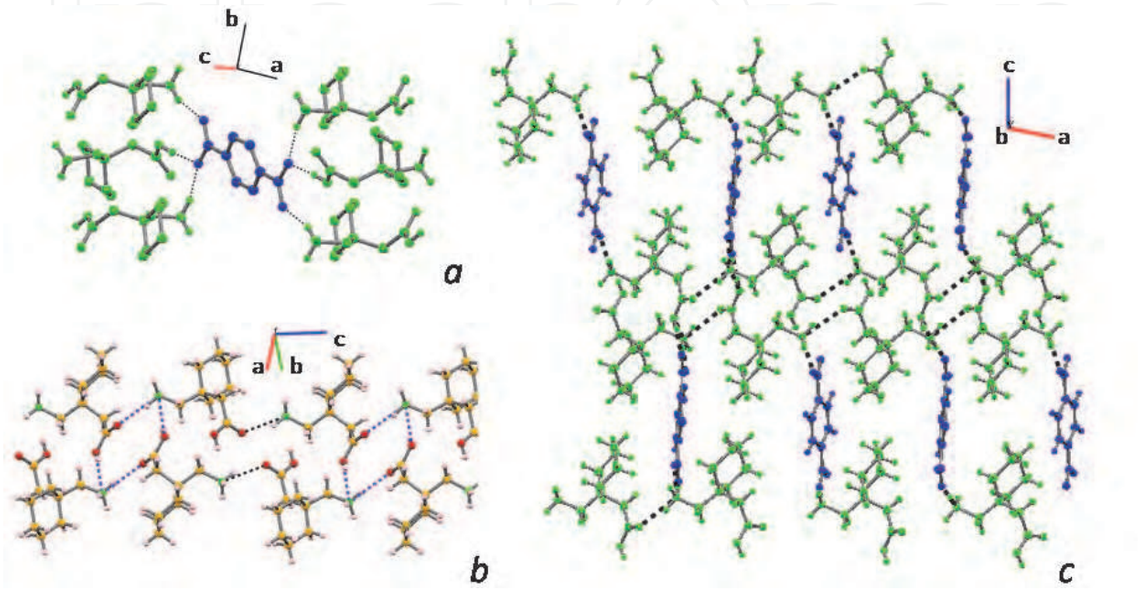

Fig. 9. Packing diagrams obtained from **4**; (a) detailed hydrogen-bonding system in **4**, (b) view showing the cationic GBP tape and depicting $R_4^4(12)$ synthons represented in blue, (c) view along *b* of the supramolecular packing where the spacer function of the coformer is clear. Color code: green – GBP; blue – coformer.

Asymmetric unit of crystalline **5** consists of one gabapentin zwitterion, one trimesic acid molecule and one water molecule. In this structure there is clear evidence that the proton transfer occurs within gabapentin, resulting in its zwitterionic form; therefore all the molecules involved in this structure are globally neutral and thus we have a hydrated co-crystal.
An intramolecular hydrogen bond is established in each gabapentin molecule [$N^+H_{GBP}\cdots O^-_{GBP}$] and gabapentin zwitterions interact among them using the amine and the carboxylate moieties, $N^+H_{GBP}\cdots O^-_{GBP}$. Both interactions are responsible for the formation of dimers based on $R_4^2(8)$ synthons (Scheme II.a).
Two of the carboxylic acid groups of trimesic acid are used to form the usual $R_2^2(8)$ synthon through $OH_{TA}\cdots O_{TA}$. The third COOH no longer maintains this typical pattern but interacts with three independent gabapentin zwitterions (Scheme II.b), two of which are involved in the previously mentioned GBP $R_4^2(8)$ dimer. In these GBP···TA interactions, C=O acts as an acceptor for one NH of gabapentin [$N^+H_{GBP}\cdots O_{TA}$]; OH works both as acceptor, from another gabapentin's amine moiety [$N^+H_{GBP}\cdots O_{TA}$], and as donor to a CO of a third gabapentin molecule [$OH_{TA}\cdots O^-_{GBP}$] (Figure 10.a). A tape of GBP zwitterionic dimers assisted by trimesic acid moieties is formed (Figure 10.b). Actually these tapes are further reinforced by water molecules as each gabapentin zwitterion interacts with three water molecules *via* $N^+H_{GBP}\cdots O_W$ and two $OH_W\cdots O^-_{GBP}$ (Scheme II.a).

The supramolecular arrangement of **5** can be described as alternated gabapentin zwitterionic ondulated chains and trimesic acid zigzag chains, with water molecules lying in the space between them (Figure 10.c). Trimesic acid besides supporting the gabapentin tapes also acts as spacer between them, similarly to compound **4**.

Comparing this structure with the three known GBP polymorphs, the intramolecular bond is similar to the one formed in polymorph IV and the $R_4^2(8)$ synthons are observed also in polymorph III. The typical $R_2^2(8)$ synthon between trimesic acid molecules is maintained in 2/3 of its interactions and it is only disrupted to establish connections with GBP zwitterions, increasing the number of hydrogen-bonds in which they both are involved.

The presence of the intramolecular bond in gabapentin zwitterions could suggest an analogue conformation of GBP molecules in this co-crystal and in polymorph IV, but this is not observed and, in fact GBP adopts different conformations.

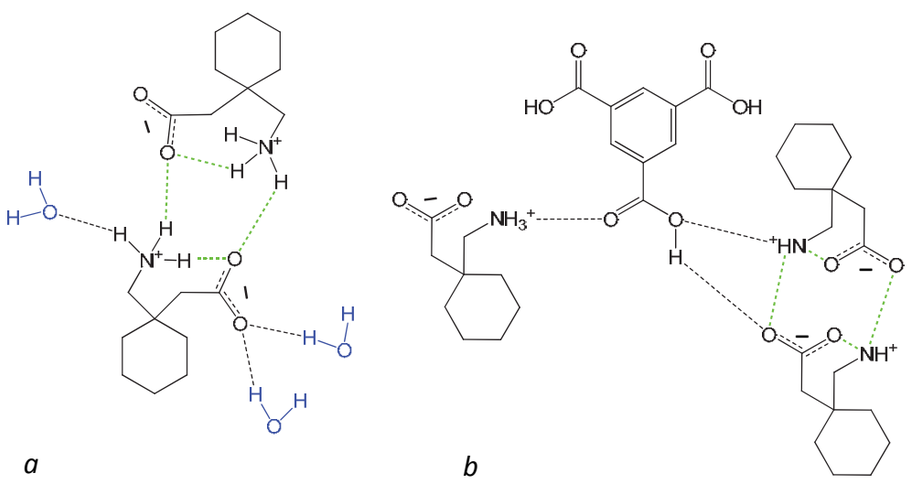

Scheme II. Main hydrogen bond interactions present in **5**.

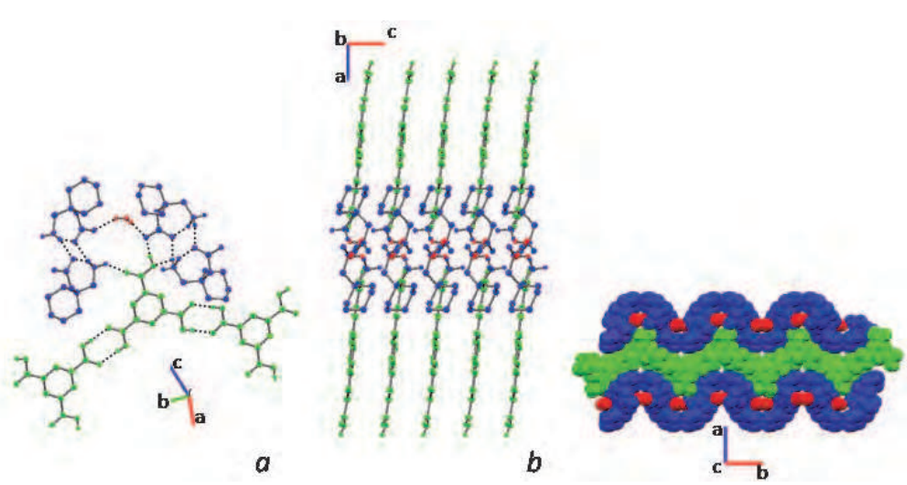

Fig. 10. Packing diagrams for co-crystal **5** (a) detailed hydrogen-bonding system in GBP:trimesic acid hydrate; (b) view along b showing both the tape made of GBP dimers assisted by water and trimesic acid spacers; (c) space filling diagram viewed along the *c*-axis. Color code: green – GBP; blue – coformer; red- water.

In both gabapentin multicomponent crystals' structures **4** and **5**, gabapentin's cyclohexane ring adopts a chair conformation in which the aminomethyl group is in an equatorial position, with the carboxymethyl group in the axial position. The relative positioning of the substituent groups is similar to the one observed in gabapentin polymorph IV; in the other two polymorphic forms of gabapentin the aminomethyl and carboxymethyl groups occupy the inverted positions (Figure 11).

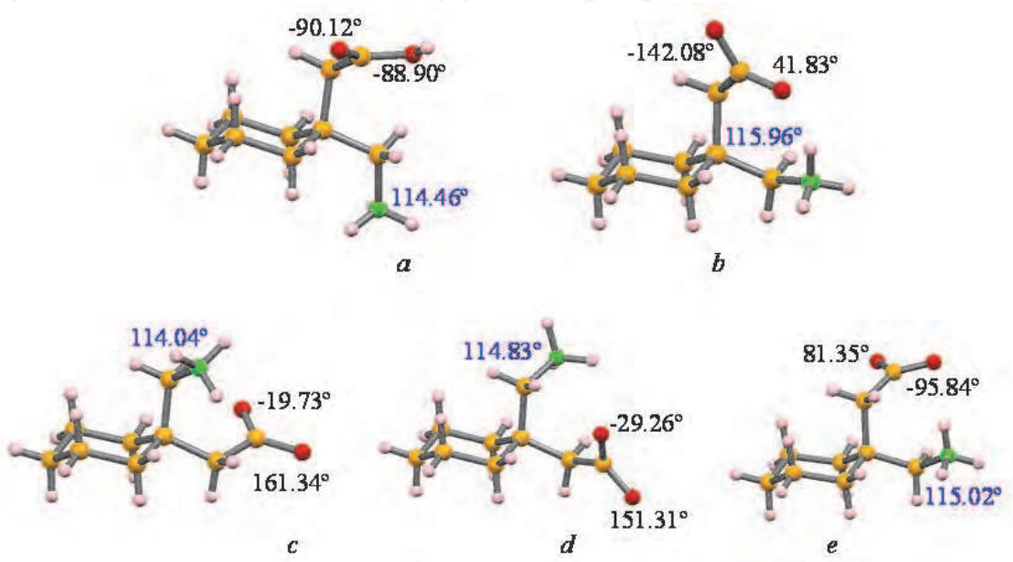

Fig. 11. A comparison of the GBP conformation in: (a) GBP:terephthalic acid molecular salt; (b) GBP:trimesic acid co-crystal; (c) GBP polymorph II; (d) GBP polymorph III; (e) GBP polymorph IV. C-C-N bond angles are given in blue and both C-C-C-O dihedral angles in black[84].

Analyzing all the unveiled multicomponent forms of gabapentin[32-34, 58, 63, 76, 79], there was no systematic behavior concerning the relative positioning of the aminomethyl and carboxymethyl substituent groups, what can lead us to conclude that this is governed by the supramolecular interactions.

As expected the carboxylate···amine interactions in GBP and the $R_2^2(8)$ in the carboxylic acids are partially disrupted and new hydrogen-bonding patterns were induced by the introduction of the coformer. Although there is proton transfer in **4** and not in **5**, in both forms GBP interacts with the acid coformer through carboxyl···carboxylate and amine···carboxyl/carboxylate synthons represented in Scheme III. The interactions *via* synthons I and II are in agreement with the results previously presented by Reddy et al[33] and Kavuru et al[86].

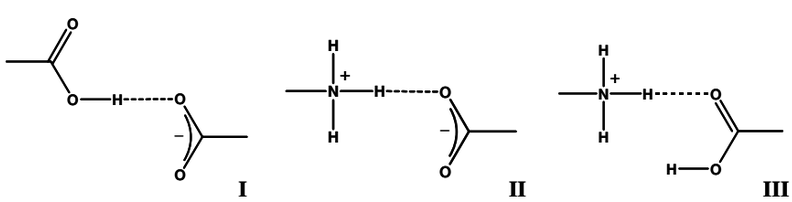

Scheme III. Main hydrogen bonded synthons observed in **4** and **5**.

Thermal studies were performed on the new crystal forms **4** and **5** and a combination of DSC, TGA and HSM data allowed some conclusions on the thermal stability of these compounds. The thermogram of **4** (Figure 12.a) is characterized by an endothermic peak at 150ºC, corresponding to the melting of the compound. The melting peak is found at a lower temperature than any of the reported polymorphic forms of gabapentin[32] and within the range obtained for other multicomponent forms[33, 34]. This peak encloses the cyclisation/ lactamization of gabapentin[32] implying water release that is observed on HSM experiments (Figure 13) and detected in TGA.

The thermogram obtained from **5** (Figure 12.b) is characterized by a wide bump between 70 and 120°C and one broad endothermic peak at 159ºC. The first peak is due to the slow release of crystallization water and the second peak encloses lactamization of gabapentin and melting as seen in **4**. Both these phenomena are supported by TGA and HSM (Figures 12 and 14).

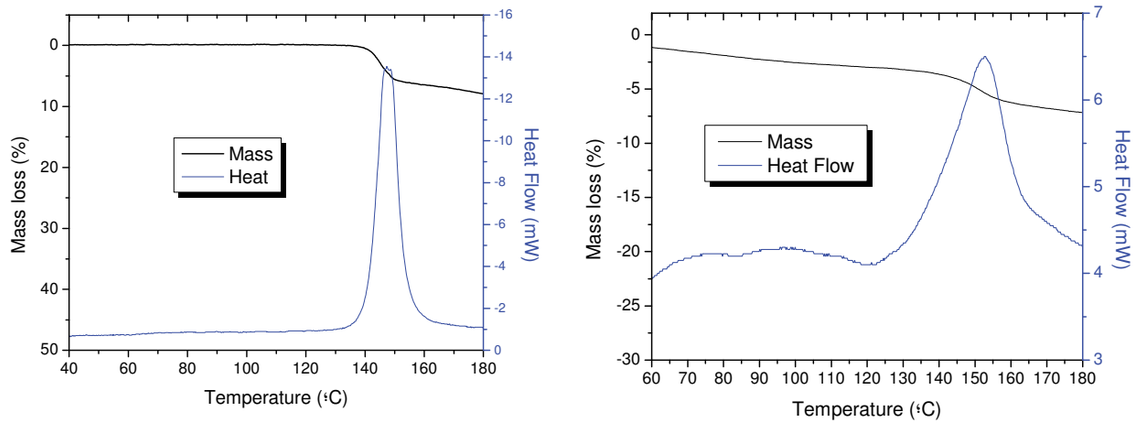

a b

Fig. 12. DSC and TGA obtained for (a) molecular salt **4**, and (b) co-crystal **5**.

As previously mentioned, HSM experiments with compounds **4** and **5** were also performed and are in agreement with what was observed in the DSC and TGA experiments and were used in the interpretation of these results.

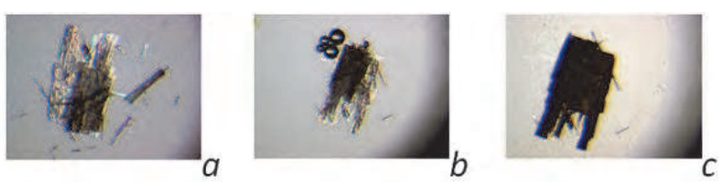

Fig. 13. HSM images for **4** at a) 25 ºC; b) 140ºC – water being released in the lactamization process; c) 144.5ºC – crystal appearance just before melting[84].

Fig. 14. HSM images for **5** at a) 25 ºC; b) 90ºC – slow release of crystallization water; c) 160ºC – lactamization and melting[84].

IR spectroscopy (Figure 15) complemented the characterization of the new crystal forms **4** and **5**. In both spectra, the presence of the NH_3^+ group is evidenced by the peaks corresponding to the symmetric and antisymmetric bending frequencies (1500 and 1610 cm^{-1}) and by the peak corresponding to the stretching frequency (2650 cm^{-1}). In **4**, the carboxylate group of the acid and the carboxylic group of the API are also well distinguished: the carbonyl band is exhibited at frequency > 1700 cm^{-1} typical of a aliphatic carboxylic group; proton transfer between the coformer and the API is confirmed by the presence of coformer carboxylate bands together with the absence of the carbonyl band typical (1680 cm^{-1}) of the terephthalic group. In **5**, although a clear identification of the carboxylate of the API and the carboxylic group of the acid is not so ascertained, it is possible to note the absence of the carboxylic moiety of gabapentin and identify, by comparison with the spectra of the pure coformer, the peak of the carboxylic moieties of trimesic acid; therefore the existence of the carboxylate in gabapentin is inferred.

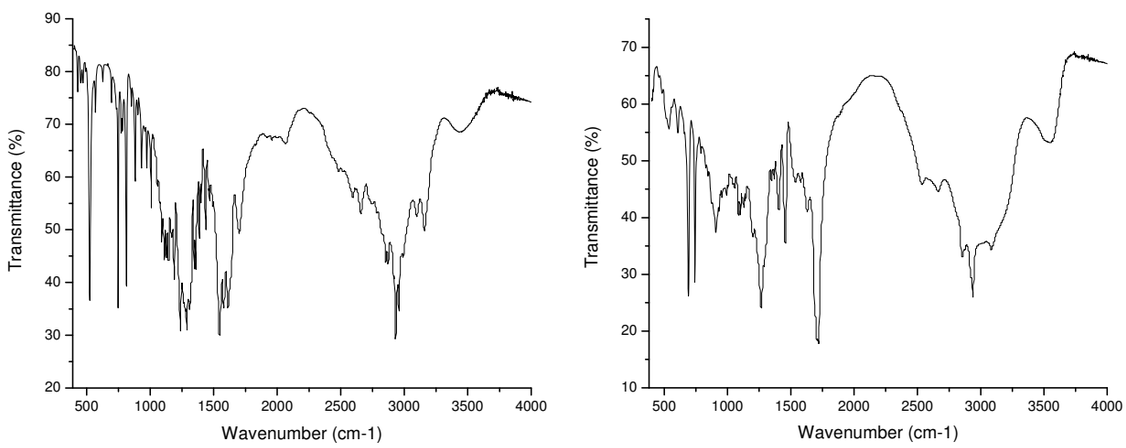

Fig. 15. IR spectra for **4** (a) and **5** (b) obtained by liquid-assisted grinding[84].

The solubility of the new multicomponent forms is lower than that for gabapentin, as desired. As previous studies on gabapentin indicate that this API is especially dependent on the pH of the environment[31], pH dependent stability of these two new forms was also studied and significant differences were found for **4** and **5**, the first being stable in quite a narrower pH range (Figures 16 and 17).

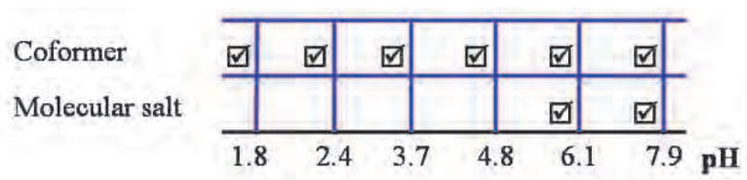

Fig. 16. pH dependent stability of **4**

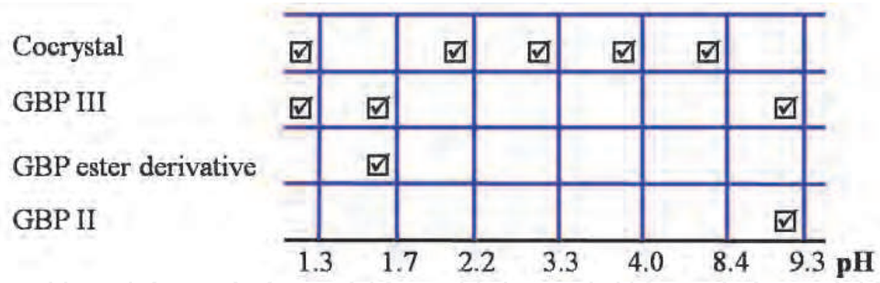

Fig. 17. pH dependent stability of **5**. [Ester derivative reported in[83]]

3. Perindopril: polymorphs and hydrates[3]

Perindopril, 2-methylpropane-2-amine-(2S,3aS,7aS)-1-[(2S)-2-[[(1S)-1-ethoxy-carbonyl-butyl] amino]propanoyl]octahydro-1H-indole-2-carboxylic acid, is an antihypertensive drug that acts through the inhibition of angiotensin converting enzyme (ACE), a zinc metalloenzyme involved in the control of blood pressure. It is effective in the treatment and prevention of several medical conditions, such as reducing blood pressure, reversing abnormalities of vascular structure and function in patients with essential hypertension, congestive heart failure, post-myocardial infarction and diabetic nephropathy[87-91]. Perindopril along with ramipril were associated with lower mortality than most other ACE inhibitors[92]. Besides the antihypertensive properties, it also comprises vasculoprotective and antithrombotic effects, playing a favourable role in terms of cardiovascular morbidity[93-99].

This API is, in fact, an acid-ester prodrug that is converted into the active diacid perindoprilat by hydrolysis promoted by the liver esterases after administration[93, 100]. It is orally administered in the form of tablets containing its 1:1 salts with erbumine (*tert*-butylamine) (Aceon®) or L-arginine (Coversyl®)[43, 101]. The perindopril L-arginine salt is equivalent to perindopril erbumine (Figure 18) but it is more stable and therefore it can be distributed to all the climatic zones without the need for specific packaging[101].

Over the last years, several forms of perindopril erbumine have been disclosed and several patents have been filed mainly based on their typical powder XRPD patterns[44, 45, 102-105]. Perindopril erbumine is known to exist in several polymorphic forms[46, 48, 102, 103, 105-107], as well as mono-, di- and sesqui-hydrated forms, characterized by XRPD, vibrational spectroscopy and thermal analysis methods[47, 108]. Also amorphous compositions have been patented[42] as well as a perindopril tosylate form[109].

Some of the different pharmacological and adverse effects exerted by ACE inhibitors may depend on the different phisicochemical (solubility, lipophilicity, acidity) and pharmacokinetic (absorption, protein binding, half-life and metabolic disposition) properties but also on their ability to penetrate and bind tissue sites[110]. Theoretical studies on p*K*a, lipophilicity, solubility, absorption and polar surface of ACE inhibitors, including perindopril, and its active metabolite, perindoprilat, have been reported[111]. In 2009, Remko presented theoretical calculations of molecular structure and stability of the arginine and erbumine salts of perindopril[43].

[3] Adapted with permission from First Crystal Structures of the Antihypertensive Drug Perindopril Erbumine: A Novel Hydrated Form and Polymorphs α and β, Vânia André, Luis Cunha-Silva, M. Teresa Duarte, and Pedro Paulo Santos, *Crystal Growth & Design*, 2011, *11* (9), pp 3703–3706, DOI: 10.1021/cg200430z. Copyright (2011) American Chemical Society".

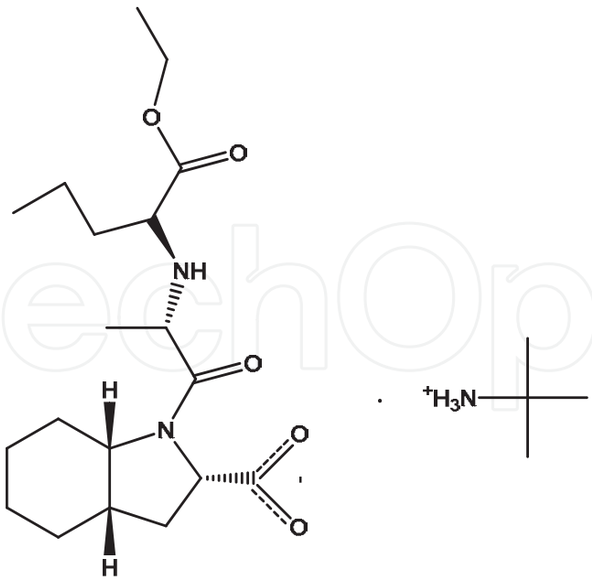

Fig. 18. Chemical diagram of perindopril erbumine salt.

Careful searches in the literature and in the Cambridge Structural Database[112] revealed that, although this API is known since 1981, until very recently only the crystal structure of perindoprilat, the pharmacologically active compound, had been determined in 1991[93]. In 2011, Remko and co-workers[41] unveiled the crystal structure of perindopril erbumine dehydrate.

Also in 2011, during a polymorphic screening of perindopril erbumine, the molecular structures of its α and β polymorphs[45, 113] have been determined by SCXRD as well as an unprecedented hydrated form of formula $(C_4H_{12}N)(C_{19}H_{31}N_2O_5)\cdot 1.25H_2O$[40, 114]. Elemental and Karl-Fischer analyses confirmed the water contents of the three forms, that were were fully characterized by XRPD, vibrational spectroscopy (ATR-FT-IR and FT-Raman) and thermal analysis methods (TGA, DSC and HSM)[40]. Furthermore, stability, solubility and dissolution profile studies were performed.

The crystal packing of polymorphic forms α and β show similar hydrogen bonding interactions involving the perindopril and the erbumine ions. Perindopril anions interact with erbumine cations in an extended NH···O hydrogen bonding network leading to a supramolecular structure with the moieties organized in a double-chain arrangement. Each erbumine cation connects with three perindopril anions *via* the amine moiety: two of them are in the same chain whereas the other perindopril belongs to the opposite chain where the positioning of the anions in their respective chains, it is possible to notice that they assume antiparallel orientations i.e., perindopril anions of one chain are rotated of 180º relatively to the anions in the adjacent chain. Consequently two related types of $C_2^2(6)$ synthons are formed in both chains that are connected among them by $D_1^1(2)$ motifs.

The NH···O hydrogen bond distances are within the ranges of 2.707 - 2.803 Å and 2.738 - 2.788 Å in α and β forms, respectively. These double-chains do not establish classical hydrogen bonds among them neither in α nor β forms.

The new 1:1:1.25 hydrated form crystallizes with a triclinic symmetry, in the P1 chiral space group. This hydrated form was obtained both by solution and by LAG, which, as previously said, has several advantages not only in the preparation process, where equally yield and

purity are obtained, but also in an environmental context[115-119]. Its asymmetric unit consists of two crystallographic independent perindopril anions, two erbumine cations and 2.5 water molecules. The CO distances in the carboxylate moiety and the location of the three hydrogen atoms in the amine moieties from the electron density map confirmed the presence of the salt.

The chiral centers in both perindopril crystallographic independent anions of the hydrated form exhibit the (S) configuration, corresponding exactly to the same configuration of the starting form α as well as of form β, what is important to assure the pharmacological activity of the API (Figure 18). The main conformational differences between these crystallographic independent anions are noted in the $-CH_2CH_2CH_3$ terminal groups (torsion angles of -58.2(4)° *vs* 175.1(9)°). The crystal packing of this hydrated form is very similar to the one described for polymorphic forms α and β, involving similar hydrogen bonding interactions between the perindopril and the erbumine ions (Figure 19). The NH···O hydrogen bond distances are within the ranges of 2.75 - 2.781 Å. The main difference between this hydrate and the polymorphs previously described is that while the double-chains do not establish classical hydrogen bonds among them neither in α nor β forms, in the hydrated form water molecules play an important role by linking adjacent chains through interactions between two crystallographically independent perindopril anions *via* the carbonyl group of one [$O_W \cdots O_{C=O}$ distance of 2.717Å] and the amine moiety of the other [$N_{N-H} \cdots O_W$ distance of 2.430Å]. Water molecules lie in the free spaces arising from the supramolecular arrangement described (Figure 19) and interact through cooperative O_W–H···O_W hydrogen bonds forming trimeric water clusters [O···O distances in the cluster: 2.644, 2.687 and 2.932 Å] (Figures 19 and 20).

Vibrational spectroscopy (FT-IR and FT-Raman) studies support the structural features unveiled by SCXRD data which are reflected in the spectra through a number of diagnostic

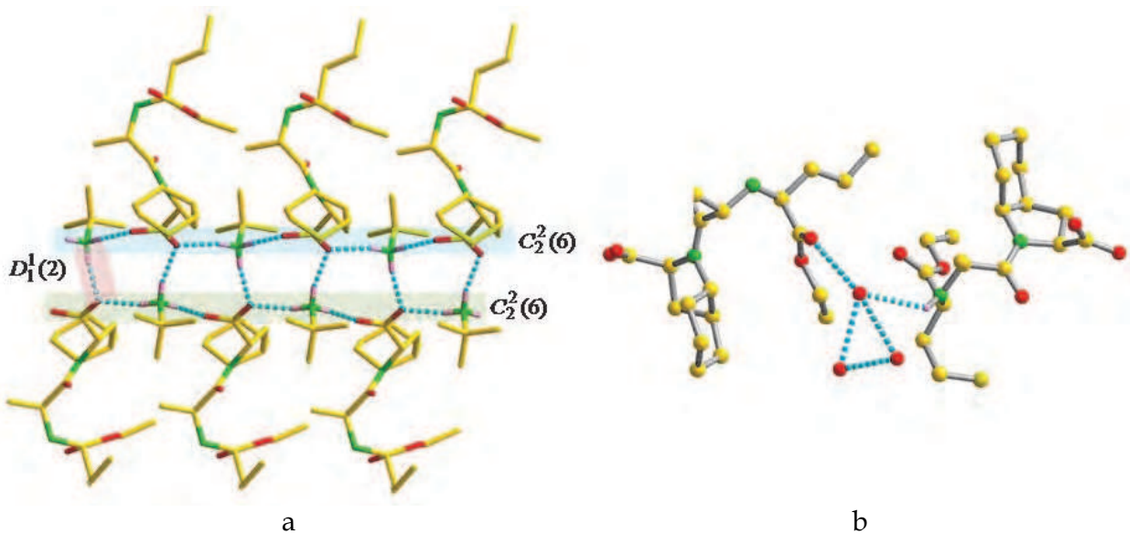

a b

Fig. 19. Crystal packing of the novel hydrated form of perindopril erbumine (1:1:1.25): (a) supramolecular arrangement with the perindopril anions and erbumine cations organized in double-chains; H bonds represented as blue dashed lines; water molecules were omitted for clarity; (b) detailed hydrogen bonding within the water cluster. Only hydrogen atoms involved in hydrogen bonding are shown, with exception of water molecules for which no hydrogen atoms are displayed[40].

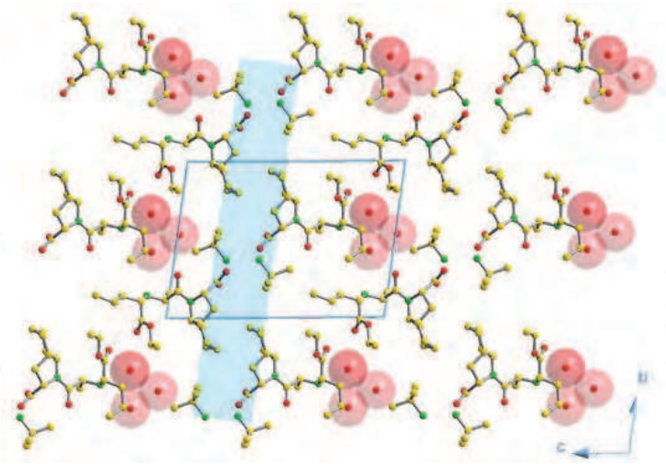

Fig. 20. Crystalline packing of the novel hydrated form of perindopril erbumine (1:1:1.25): Double-chain array formed by $C_2^2(6)$ and $D_1^1(2)$ motifs is highlighted in blue[40].

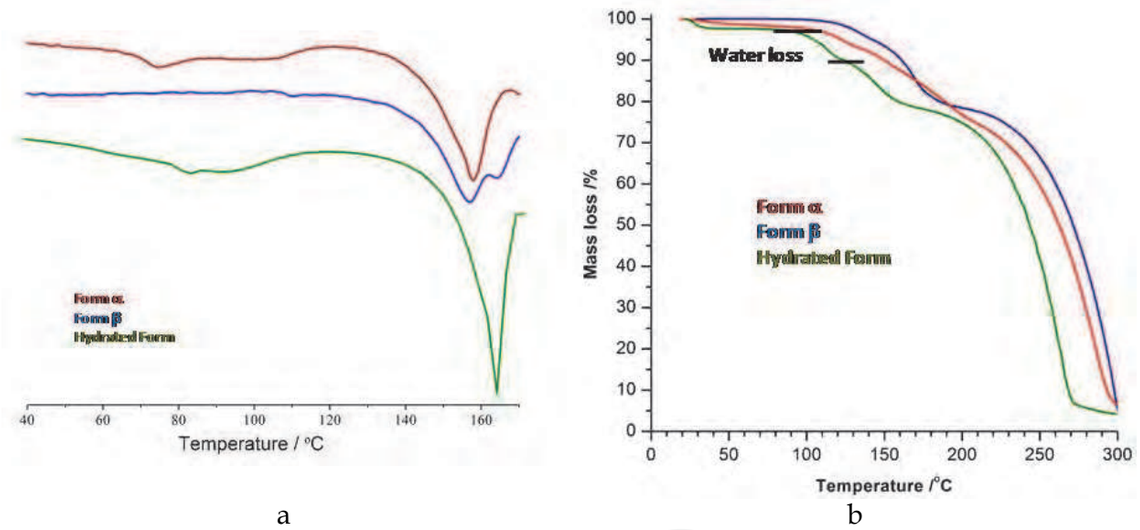

a b

Fig. 21. (a) DSC and (b) TGA pattern for all the forms of perindopril erbumine discussed.

bands (Figure 21). In particular the strong bands in the range of 3200-2600 cm^{-1} of the FT-Raman spectra are attributed to the υ_s(C–H) and υ_s(N–H) stretching vibrational modes diagnosing the presence of NH and NH_3^+ groups in the perindopril and erbumine cation, respectively. The strong bands around 1642, 1569 cm^{-1} and 1387 cm^{-1} (observed in both the FT-IR and FT-Raman spectra) are assigned to the $\upsilon_s(COO^-)$ and $\upsilon_{as}(COO^-)$ respectively, confirming the deprotonation of the carboxylic acid group. Contrasting with the FT-IR spectra of forms α and β, the spectrum of the hydrated form in the 3200-2600 cm^{-1} range reflects the presence of crystallization water molecules involved in well defined hydrogen bonds, by the presence of resolved peaks.

The combination of data obtained from DSC, TGA and HSM indicates that the novel hydrated form is stable until approximately 80°C, temperature at which a peak is observed in the DSC (Figure 21.a), a smooth mass loss is detected in the TGA (Figure 21.b) and bubbles start to appear in the HSM. The water loss occurs from this temperature until

approximately 120°C. At 164ºC melting and decomposition take place. TGA for forms α and β reveals that there is no mass loss before 120°C, confirming the absence of water in both these forms.
The new 1:1:1.25 hydrate has shown to be as stable on shelf as form α for eighteen months and water slurry experiments revealed that it as a thermodynamically stable form. It has also shown to have a similar dissolution profile (Figure 22) as the commercially available drug and to be slightly more soluble in water than the α form[40].

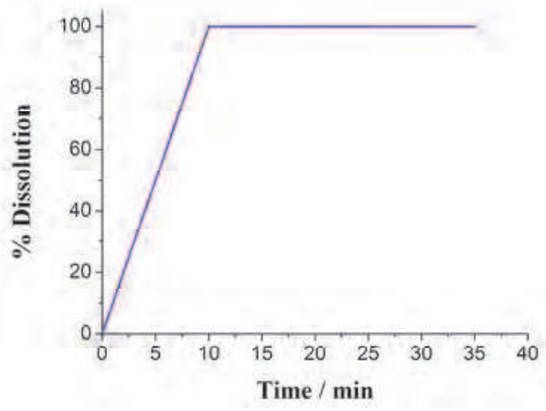

Fig. 22. Dissolution profile for the 1:1:1.25 hydrated form.

A probable reason for this is the enhanced stability provided by the presence of the water molecules linking the erbumine-perindopril double chains. Analysis of crystal structure has again proven to be quite important for the establishment of the intermolecular interactions responsible for the supramolecular arrangement and thus the physicochemical properties of APIs.

4. Concluding remarks

Over the last two decades crystal engineering, a key tool for the design of new crystal forms, has made possible the synthesis of novel pharmaceutical materials as well as molecular level control of crystallization and phase transformations. Advances in crystal engineering and supramolecular chemistry invite us to consider new perspectives and perhaps definitions of the various solid-state forms that the same and/or different molecules may adopt in terms of molecular assemblies and architectures.
Pharmaceutical co-crystals have proven to offer potential benefits of superior efficacy, solubility and stability in drug formulation. It seems reasonable to assert that co-crystal approaches should be considered routinely as part of a broader set of form and formulation explorations to achieve the best possible drug products. Although the interest in co-crystals and polymorphs and their utility is obvious, identifying and implementing an efficient discovery and control method remains a challenge.

5. Acknowledgements

The authors acknowledge Fundação para a Ciência e a Tecnologia, MCTES, Portugal, for funding the Project POCI/QUI/58791/2004, PEst-OE/QUI/UI0100 /2011, and the Ph.D. Grant SFRH/40474/2007 (V.A.).

6. References

[1] H. T. Wu, G. Kaur, and G. L. Griffiths, An improved synthesis of a fluorescent gabapentin-choline conjugate for single molecule detection. *Tetrahedron Letters*, 50, (2009):2100.

[2] R. D. B. Walsh, M. W. Bradner, S. Fleischman, L. A. Morales, B. Moulton, N. Rodriguez-Hornedo, and M. J. Zaworotko, Crystal engineering of the composition of pharmaceutical phases. *Chemical Communications*, (2003):186.

[3] S. L. Childs, L. J. Chyall, J. T. Dunlap, V. N. Smolenskaya, B. C. Stahly, and G. P. Stahly, Crystal engineering approach to forming co-crystals of amine hydrochlorides with organic acids. Molecular complexes of fluoxetine hydrochloride with benzoic, succinic, and fumaric acids. *Journal of the American Chemical Society*, 126, (2004):13335.

[4] O. Almarsson and M. J. Zaworotko, Crystal engineering of the composition of pharmaceutical phases. Do pharmaceutical co-crystals represent a new path to improved medicines? *Chemical Communications*, (2004):1889.

[5] N. Shan and M. J. Zaworotko, The role of co-crystals in pharmaceutical science. *Drug Discovery Today*, 13, (2008):440.

[6] P. Vishweshwar, J. A. McMahon, J. A. Bis, and M. J. Zaworotko, Pharmaceutical co-crystal. *Journal of Pharmaceutical Sciences*, 95, (2006):499.

[7] J. F. Remenar, S. L. Morissette, M. L. Peterson, B. Moulton, J. M. MacPhee, H. R. Guzman, and O. Almarsson, Crystal engineering of novel co-crystals of a triazole drug with 1,4-dicarboxylic acids. *Journal of the American Chemical Society*, 125, (2003):8456.

[8] D. P. McNamara, S. L. Childs, J. Giordano, A. Iarriccio, J. Cassidy, M. S. Shet, R. Mannion, E. O'Donnell, and A. Park, Use of a glutaric acid co-crystal to improve oral bioavailability of a low solubility API. *Pharmaceutical Research*, 23, (2006):1888.

[9] T. Friscic, A. V. Trask, W. D. S. Motherwell, and W. Jones, Guest-directed assembly of caffeine and succinic acid into topologically different heteromolecular host networks upon grinding. *Crystal Growth & Design*, 8, (2008):1605.

[10] M. B. Hickey, M. L. Peterson, L. A. Scoppettuolo, S. L. Morrisette, A. Vetter, H. Guzman, J. F. Remenar, Z. Zhang, M. D. Tawa, S. Haley, M. J. Zaworotko, and O. Almarsson, Performance comparison of a co-crystal of carbamazepine with marketed product. *European Journal of Pharmaceutics and Biopharmaceutics*, 67, (2007):112.

[11] J. F. Remenar, M. L. Peterson, P. W. Stephens, Z. Zhang, Y. Zimenkov, and M. B. Hickey, Celecoxib : Nicotinamide dissociation: Using excipients to capture the co-crystal's potential. *Molecular Pharmaceutics*, 4, (2007):386.

[12] S. G. Fleischman, S. S. Kuduva, J. A. McMahon, B. Moulton, R. D. B. Walsh, N. Rodriguez-Hornedo, and M. J. Zaworotko, Crystal engineering of the composition of pharmaceutical phases: Multiple-component crystalline solids involving carbamazepine. *Crystal Growth & Design*, 3, (2003):909.

[13] J. A. McMahon, J. A. Bis, P. Vishweshwar, T. R. Shattock, O. L. McLaughlin, and M. J. Zaworotko, Crystal engineering of the composition of pharmaceutical phases. 3. Primary amide supramolecular heterosynthons and their role in the design of pharmaceutical co-crystals. *Zeitschrift fur Kristallographie*, 220, (2005):340.

[14] K. Shiraki, N. Takata, R. Takano, Y. Hayashi, and K. Terada, Dissolution improvement and the mechanism of the improvement from co-crystallization of poorly water-soluble compounds. *Pharmaceutical Research*, 25, (2008):2581.

[15] M. K. Stanton, S. Tufekcic, C. Morgan, and A. Bak, Drug Substance and Former Structure Property Relationships in 15 Diverse Pharmaceutical Co-Crystals. *Crystal Growth & Design*, 9, (2009):1344.

[16] A. V. Trask, W. D. S. Motherwell, and W. Jones, Pharmaceutical co-crystallization: Engineering a remedy for caffeine hydration. *Crystal Growth & Design*, 5, (2005):1013.

[17] A. V. Trask, W. D. S. Motherwell, and W. Jones, Physical stability enhancement of theophylline via co-crystallization. *International Journal of Pharmaceutics*, 320, (2006):114.

[18] A. Bak, A. Gore, E. Yanez, M. Stanton, S. Tufekcic, R. Syed, A. Akrami, M. Rose, S. Surapaneni, T. Bostick, A. King, S. Neervannan, D. Ostovic, and A. Koparkar, The co-crystal approach to improve the exposure of a water-insoluble compound: AMG 517 sorbic acid co-crystal characterization and pharmacokinetics. *Journal of Pharmaceutical Sciences*, 97, (2008):3942.

[19] A. M. Chen, M. E. Ellison, A. Peresypkin, R. M. Wenslow, N. Variankaval, C. G. Savarin, T. K. Natishan, D. J. Mathre, P. G. Dormer, D. H. Euler, R. G. Ball, Z. X. Ye, Y. L. Wang, and I. Santos, Development of a pharmaceutical co-crystal of a monophosphate salt with phosphoric acid. *Chemical Communications*, (2007):419.

[20] N. Variankaval, R. Wenslow, J. Murry, R. Hartman, R. Helmy, E. Kwong, S. D. Clas, C. Dalton, and I. Santos, Preparation and solid-state characterization of nonstoichiometric co-crystals off a phosphodiesterase-IV inhibitor annul L-tartaric acid. *Crystal Growth & Design*, 6, (2006):690.

[21] S. L. Childs and K. I. Hardcastle, Co-crystals of chlorzoxazone with carboxylic acids. *Crystengcomm*, 9, (2007):363.

[22] C. B. Aakeroy, M. E. Fasulo, and J. Desper, Co-crystal or salt: Does it really matter? *Molecular Pharmaceutics*, 4, (2007):317.

[23] F. H. Allen, The Cambridge Structural Database: a quarter of a million crystal structures and rising. *Acta Crystallographica Section B-Structural Science*, 58, (2002):380.

[24] W. W. Porter, S. C. Elie, and A. J. Matzger, Polymorphism in carbamazepine co-crystals. *Crystal Growth & Design*, 8, (2008):14.

[25] S. Karki, T. Friscic, and W. Jones, Control and interconversion of co-crystal stoichiometry in grinding: stepwise mechanism for the formation of a hydrogen-bonded co-crystal. *Crystengcomm*, 11, (2009):470.

[26] T. Friscic, S. L. Childs, S. A. A. Rizvi, and W. Jones, The role of solvent in mechanochemical and sonochemical co-crystal formation: a solubility-based approach for predicting co-crystallisation outcome. *Crystengcomm*, 11, (2009):418.

[27] T. Friscic, L. Fabian, J. C. Burley, W. Jones, and W. D. S. Motherwell, Exploring co-crystal - co-crystal reactivity via liquid-assisted grinding: the assembling of racemic and dismantling of enantiomeric co-crystals. *Chemical Communications*, (2006):5009.

[28] S. Karki, T. Friscic, W. Jones, and W. D. S. Motherwell, Screening for pharmaceutical co-crystal hydrates via neat and liquid-assisted grinding. *Molecular Pharmaceutics*, 4, (2007):347.

[29] D. Braga, L. Maini, G. de Sanctis, K. Rubini, F. Grepioni, M. R. Chierotti, and R. Gobetto, Mechanochemical preparation of hydrogen-bonded adducts between the diamine 1,4-diazabicyclo [2.2.2] octane and dicarboxylic acids of variable chain length: An x-ray diffraction and solid-state NMR study. *Chemistry-A European Journal*, 9, (2003):5538.

[30] D. Braga and F. Grepioni, Making crystals from crystals: a green route to crystal engineering and polymorphism. *Chemical Communications*, (2005):3635.

[31] V. Andre, M. M. Marques, M. F. M. da Piedade, and M. T. Duarte, An ester derivative of the drug gabapentin: pH dependent crystal stability. *Journal of Molecular Structure*, 973, (2010):173.

[32] D. Braga, F. Grepioni, L. Maini, K. Rubini, M. Polito, R. Brescello, L. Cotarca, M. T. Duarte, V. Andre, and M. F. M. Piedade, Polymorphic gabapentin: thermal behaviour, reactivity and interconversion of forms in solution and solid-state. *New Journal of Chemistry*, 32, (2008):1788.

[33] L. S. Reddy, S. J. Bethune, J. W. Kampf, and N. Rodriguez-Hornedo, Co-crystals and Salts of Gabapentin: pH Dependent Co-crystal Stability and Solubility. *Crystal Growth & Design*, 9, (2009):378.

[34] M. Wenger and J. Bernstein, An alternate crystal form of gabapentin: A co-crystal with oxalic acid. *Crystal Growth & Design*, 8, (2008):1595.

[35] V. Andre, D. Braga, F. Grepioni, and M. T. Duarte, Crystal Forms of the Antibiotic 4-Aminosalicylic Acid: Solvates and Molecular Salts with Dioxane, Morpholine, and Piperazine. *Crystal Growth & Design*, 9, (2009):5108.

[36] V. Andre, D. Braga, F. Grepioni, and M. Duarte, Crystal Forms of the Antibiotic 4-Aminosalicylic Acid: Solvates and Molecular Salts with Dioxane, Morpholine, and Piperazine. *Crystal Growth & Design*, 9, (2009):5108.

[37] F. P. A. Fabbiani, D. R. Allan, A. Dawson, W. I. F. David, P. A. McGregor, I. D. H. Oswald, S. Parsons, and C. R. Pulham, Pressure-induced formation of a solvate of paracetamol. *Chemical Communications*, (2003):3004.

[38] I. D. H. Oswald, D. R. Allan, P. A. McGregor, W. D. S. Motherwell, S. Parsons, and C. R. Pulham, The formation of paracetamol (acetaminophen) adducts with hydrogen-bond acceptors. *Acta Crystallographica Section B-Structural Science*, 58, (2002):1057.

[39] I. D. H. Oswald, W. D. S. Motherwell, S. Parsons, and C. R. Pulham, A paracetamol-morpholine adduct. *Acta Crystallographica Section E-Structure Reports Online*, 58, (2002):O1290.

[40] V. n. André, L. s. Cunha-Silva, M. T. Duarte, and P. P. Santos, First Crystal Structures of the Antihypertensive Drug Perindopril Erbumine: A Novel Hydrated Form and Polymorphs α and β. *Crystal Growth & Design*, 11, (2011):3703.

[41] M. Remko, J. Bojarska, P. Jezko, L. Sieron, A. Olczak, and W. Maniukiewicz, Crystal and molecular structure of perindopril erbumine salt. *Journal of Molecular Structure*, 997, (2011):103.

[42] P. Gupta, N. Bhandari, S. Gore, M. K. Pananchukunnath, and I. Bhushan, IN200802491-I4, 2010.

[43] M. Remko, Molecular structure and stability of perindopril erbumine and perindopril L-arginine complexes. *European Journal of Medicinal Chemistry*, 44, (2009):101.

[44] A. Kumar, S. R. Soudagar, A. Mathur, S. T. Gunjal, N. B. Panda, and D. U. Jadhav, EP1987828-A1, 2008.

[45] A. Kumar, S. R. Soudagar, A. Mathur, and N. B. Panda, US2008183011-A1; EP1964836-A2; IN200601843-I3; EP1964836-A3, 2008.
[46] A. Ujagare, D. A. Kochrekar, and P. Sarjekar, WO2007017894-A2, 2007.
[47] A. Ujagare, D. A. Kochrekar, and P. Sarjekar, WO2007017893-A2, 2007.
[48] C. Straessler, V. Lellek, R. Faessler, R. Fassler, C. Strassler, C. Strossler, R. Fossler, S. Christoph, L. Vit, and F. Roger, WO2004113293-A1; NO200600256-A; EP1636185-A1; AU2004249345-A1; BR200411966-A; KR2006035636-A; MX2005013811-A1; CN1812971-A; JP2007507418-W; US2007135512-A1; ZA200600655-A; CN100395235-C; CN101333181-A; NZ544160-A; AU2004249345-B2; AU2004249345-B8; MX268989-B; US7705046-B2; US2010160404-A1, 2005.
[49] D. Braga, F. Grepioni, V. Andre, and M. T. Duarte, Drug-containing coordination and hydrogen bonding networks obtained mechanochemically. *Crystengcomm*, 11, (2009):2618.
[50] A. A. Jensen, J. Mosbacher, S. Elg, K. Lingenhoehl, T. Lohmann, T. N. Johansen, B. Abrahamsen, J. P. Mattsson, A. Lehmann, B. Bettler, and H. Brauner-Osborne, The anticonvulsant gabapentin (Neurontin) does not act through gamma-aminobutyric acid-B receptors. *Molecular Pharmacology*, 61, (2002):1377.
[51] C. P. Taylor, Emerging Perspectives on the Mechanism of Action of Gabapentin. *Neurology*, 44, (1994):10.
[52] C. P. Taylor, N. S. Gee, T. Z. Su, J. D. Kocsis, D. F. Welty, J. P. Brown, D. J. Dooley, P. Boden, and L. Singh, A summary of mechanistic hypotheses of gabapentin pharmacology. *Epilepsy Research*, 29, (1998):233.
[53] C. M. Santi, F. S. Cayabyab, K. G. Sutton, J. E. McRory, J. Mezeyova, K. S. Hamming, D. Parker, A. Stea, and T. P. Snutch, Differential inhibition of T-type calcium channels by neuroleptics. *Journal of Neuroscience*, 22, (2002):396.
[54] A. C. Errington, T. Stohr, and G. Lees, Voltage gated ion channels: Targets for anticonvulsant drugs. *Current Topics in Medicinal Chemistry*, 5, (2005):15.
[55] A. B. Ettinger and C. E. Argoff, Use of Antiepileptic drugs for nonepileptic conditions: psychiatric disorders and chronic pain. *Neurotherapeutics*, 4, (2007):75.
[56] A. S. Kato and D. S. Bredt, Pharmacological regulation of ion channels by auxiliary subunits. *Current Opinion in Drug Discovery & Development*, 10, (2007):565.
[57] E. Eisenberg, Y. River, A. Shifrin, and N. Krivoy, Antiepileptic drugs in the treatment of neuropathic pain. *Drugs*, 67, (2007):1265.
[58] K. Ananda, S. Aravinda, P. G. Vasudev, K. M. P. Raja, H. Sivaramakrishnan, K. Nagarajan, N. Shamala, and P. Balaram, Stereochemistry of gabapentin and several derivatives: Solid state conformations and solution equilibria. *Current Science*, 85, (2003):1002.
[59] F. Henle, J. Leemhuis, C. Schmid, T. J. Feuerstein, and D. K. Meyer, Gabapentin-lactam induces the formation of dendritic branches in cultured hippocampal neurons. *Naunyn-Schmiedebergs Archives of Pharmacology*, 369, (2004):342.
[60] F. Henle, J. Leemhuis, C. Fischer, H. H. Bock, K. Lindemeyer, T. J. Feuerstein, and D. K. Meyer, Gabapentin-lactam induces dendritic filopodia and motility in cultured hippocampal neurons. *Journal of Pharmacology and Experimental Therapeutics*, 319, (2006):181.

[61] P. Revill, J. Bolos, N. Serradell, and M. Bayes, Gabapentin enacarbil. Treatment of restless legs syndrome, treatment of postherpetic neuralgia, treatment of neuropathic pain. *Drugs of the Future*, 31, (2006):771.

[62] K. C. Cundy, T. Annamalai, L. Bu, J. De Vera, J. Estrela, W. Luo, P. Shirsat, A. Torneros, F. M. Yao, J. Zou, R. W. Barrett, and M. A. Gallop, XP13512 [(+/-)-1-([(alpha-isobutanoyloxyethoxy)carbonyl] aminomethyl)-1-cyclohexane acetic acid], a novel gabapentin prodrug: II. Improved oral bioavailability, dose proportionality, and colonic absorption compared with gabapentin in rats and monkeys. *Journal of Pharmacology and Experimental Therapeutics*, 311, (2004):324.

[63] J. A. Ibers, Gabapentin and gabapentin monohydrate. *Acta Crystallographica Section C-Crystal Structure Communications*, 57, (2001):641.

[64] H. A. Reece and D. C. Levendis, Polymorphs of gabapenitin. *Acta Crystallographica Section C-Crystal Structure Communications*, 64, (2008):O105.

[65] D. E. Butter and B. J. Greenman, US Patent, No. 4 894 476, 1990.

[66] G. Satzinger, J. Hartenstein, M. Herrmann, and W. Heldt, US Patent, No. 4 024 175, 1977.

[67] J. A. Ibers, Gabapentin and gabapentin monohydrate. *Acta Crystallographica, Section C: Crystal Structure Communications*, C57, (2001):641.

[68] D. Braga, F. Grepioni, L. Maini, K. Rubini, M. Polito, R. Brescello, L. Cotarca, M. Duarte, V. Andre, and M. Piedade, Polymorphic gabapentin: thermal behaviour, reactivity and interconversion of forms in solution and solid-state. *New Journal of Chemistry*, 32, (2008):1788.

[69] P. Pesachovich, C. Singer, and G. Pilarski, US Patent, No. 6 255 526 B1, 2001.

[70] H. A. Reece and D. C. Levendis, Polymorphs of gabapentin. *Acta Crystallographica Section C*, 64, (2008):o105.

[71] L. R. Chen, S. R. Babu, C. J. Calvitt, and B. Tobias, US Patent, No. 6 800 782 B2, 2004.

[72] J. Bosh Lladò, R. G. Cruz, E. M. Grau, and M. d. C. O. Miguel, US Patent, No. 6 521 787 B1, 2003.

[73] Y. Kumar, C. H. Khanduri, K. K. Ganagakhedkar, R. Chakraborty, h. N. Dorwal, A. Rohtagi, and A. K. Panda, International Publication Number Patent, No. WO 2004/106281 A1, 2004.

[74] A. Cutrignelli, N. Denora, A. Lopedota, A. Trapani, V. Laquintana, A. Latrofa, G. Trapani, and G. Liso, Comparative effects of some hydrophilic excipients on the rate of gabapentin and baclofen lactamization in lyophilized formulations. *International Journal of Pharmaceutics*, 332, (2007):98.

[75] A. S. Kearney, S. C. Mehta, and G. W. Radebaugh, The effect of cyclodextrins on the rate of intramolecular lactamization of gabapentin in aqueous solution. *International Journal of Pharmaceutics*, 78, (1992):25.

[76] P. G. Vasudev, S. Aravinda, K. Ananda, S. D. Veena, K. Nagarajan, N. Shamala, and P. Balaram, Crystal Structures of a New Polymorphic Form of Gabapentin Monohydrate and the E and Z Isomers of 4-Tertiarybutylgabapentin. *Chemical Biology & Drug Design*, 73, (2009):83.

[77] D. E. Butler and B. J. Greenman, EP340677-A2; AU8932678-A; DK8902126-A; FI8902067-A; JP2011546-A; US4894476-A; US4960931-A; CA1306755-C; EP340677-B1; DE68912819-E; ES2061774-T3; IE62958-B; JP2619951-B2; DK200200056-A; DK175127-B; DK175400-B.

[78] L. J. Bosch, M. D. C. Onrubia Miguel, L. E. Pagans, M. C. Onrubia Miguel, L. J. Bosch, M. M. C. Onrubia, and L. E. Pagans, WO200064857-A; EP1174418-A; WO200064857-A1; AU200035592-A; EP1174418-A1; ES2164527-A1; HU200200741-A2; US6528682-B1; ES2164527-B1; EP1174418-B1; DE60007734-E; ES2213571-T3; IN200101052-P2; IL145920-A.

[79] J. P. Jasinski, R. J. Butcher, H. S. Yathirajan, L. Mallesha, K. N. Mohana, and B. Narayana, Crystal Structure of a Second Polymorph of Gabapentin Hydrochloride Hemihydrate with a Three-Center Bifurcated Hydrogen Bond. *JOURNAL OF CHEMICAL CRYSTALLOGRAPHY*, 39, (2009):777.

[80] S. Chava, S. R. Gorantla, V. S. K. Indukuri, V. S. K. Indukurl, C. Satyanarayana, G. S. Ramanjaneyulu, and I. V. Kumar, WO2004093780-A2; EP1615875-A2; US2006235079-A1; US7439387-B2.

[81] F. P. A. Fabbiani, D. C. Levendis, G. Buth, W. F. Kuhs, N. Shankland, and H. Sowa, Searching for novel crystal forms by in situ high-pressure crystallisation: the example of gabapentin heptahydrate. *Crystengcomm*, 12, (2010):2354.

[82] D. Braga, F. Grepioni, L. Maini, R. Brescello, and L. Cotarca, Simple and quantitative mechanochemical preparation of the first zinc and copper complexes of the neuroleptic drug gabapentin. *Crystengcomm*, 10, (2008):469.

[83] V. Andre, M. Marques, M. da Piedade, and M. Duarte, An ester derivative of the drug gabapentin: pH dependent crystal stability. *Journal of Molecular Structure*, 973, (2010):173.

[84] V. Andre, A. Fernandes, P. P. Santos, and M. T. Duarte, On the Track of New Multicomponent Gabapentin Crystal Forms: Synthon Competition and pH Stability. *Crystal Growth & Design*, 11, (2011):2325.

[85] R. Williams, pKa Data Compiled by R. Williams. http://research.chem.psu.edu/brpgroup/pKa_compilation.pdf.

[86] P. Kavuru, D. Aboarayes, K. K. Arora, H. D. Clarke, A. Kennedy, L. Marshall, T. T. Ong, J. Perman, T. Pujari, L. Wojtas, and M. J. Zaworotko, Hierarchy of Supramolecular Synthons: Persistent Hydrogen Bonds Between Carboxylates and Weakly Acidic Hydroxyl Moieties in Co-crystals of Zwitterions. *Crystal Growth & Design*, 10, (2010):3568.

[87] L. H. Opie, Inhibition of the Cerebral Renin-Angiotensin System to Limit Cognitive Decline in Elderly Hypertensive Persons. *Cardiovascular Drugs and Therapy*, 25, (2011):277.

[88] L. Opie, T. Dalby, and D. P. Naidoo, Perindopril (Coversyl) prevents cardiovascular death and MI in coronary disease patients regardless of their cardiovascular risk. *Cardiovascular journal of South Africa : official journal for Southern Africa Cardiac Society [and] South African Society of Cardiac Practitioners*, 14, (2003):277.

[89] J. Wong, R. A. Patel, and P. R. Kowey, The clinical use of angiotensin-converting enzyme inhibitors. *Progress in Cardiovascular Diseases*, 47, (2004):116.

[90] M. E. Bertrand, Provision of cardiovascular protection by ACE inhibitors: a review of recent trials. *Current Medical Research and Opinion*, 20, (2004):1559.

[91] S. Laurent, Clinical benefit of very-low-dose perindopril-indapamide combination in hypertension. *Journal of Hypertension*, 19, (2001):S9.

[92] L. Pilote, M. Abrahamowicz, E. Rodrigues, M. J. Eisenberg, and E. Rahme, Mortality rates in elderly patients who take different angiotensin-converting enzyme

inhibitors after acute myocardial infarction: A class effect? *Annals of Internal Medicine*, 141, (2004):102.

[93] C. Pascard, J. Guilhem, M. Vincent, G. Remond, B. Portevin, and M. Laubie, CONFIGURATION AND PREFERENTIAL SOLID-STATE CONFORMATIONS OF PERINDOPRILAT (S-9780) - COMPARISON WITH THE CRYSTAL-STRUCTURES OF OTHER ACE INHIBITORS AND CONCLUSIONS RELATED TO STRUCTURE-ACTIVITY-RELATIONSHIPS. *Journal of Medicinal Chemistry*, 34, (1991):663.

[94] A. Remkova and H. Kratochvil'ova, Effect of the angiotensin-converting enzyme inhibitor perindopril on haemostasis in essential hypertension. *Blood Coagulation & Fibrinolysis*, 11, (2000):641.

[95] A. Okrucka, J. Pechan, and H. Kratochvilova, Effects of the angiotensin-converting enzyme (ACE) inhibitor perindopril on endothelial and platelet functions in essential hypertension. *Platelets*, 9, (1998):63.

[96] A. Remkova, H. Kratochvil'ova, and J. Durina, Impact of the therapy by renin-angiotensin system targeting antihypertensive agents perindopril versus telmisartan on prothrombotic state in essential hypertension. *Journal of Human Hypertension*, 22, (2008):338.

[97] D. Neglia, E. Fommei, A. Varela-Carver, M. Mancini, S. Ghione, M. Lombardi, P. Pisani, H. Parker, G. D'Amati, L. Donato, and P. G. Camici, Perindopril and indapamide reverse coronary microvascular remodelling and improve flow in arterial hypertension. *Journal of Hypertension*, 29, (2011):364.

[98] S. Laurent, Predictors of cardiovascular mortality and morbidity in hypertension. *Current medical research and opinion*, 21 Suppl 5, (2005):S7.

[99] A. Remkova and M. Remko, The Role of Renin-Angiotensin System in Prothrombotic State in Essential Hypertension. *Physiological Research*, 59, (2010):13.

[100] B. Lecocq, C. Funckbrentano, V. Lecocq, A. Ferry, M. E. Gardin, M. Devissaguet, and P. Jaillon, INFLUENCE OF FOOD ON THE PHARMACOKINETICS OF PERINDOPRIL AND THE TIME COURSE OF ANGIOTENSIN-CONVERTING ENZYME-INHIBITION IN SERUM. *Clinical Pharmacology & Therapeutics*, 47, (1990):397.

[101] E. Telejko, Perindopril arginine: benefits of a new salt of the ACE inhibitor perindopril. *Current Medical Research and Opinion*, 23, (2007):953.

[102] R. Rucman, WO2005068490-A1; EP1709066-A1; EP1709066-B1; DE602005009319-E; EP2003142-A1; RU2372353-C2, 2005.

[103] R. Rucman, WO2005068425-A1; EP1713771-A1; RU2387641-C2, 2005.

[104] R. Rucman and P. Zupet, WO2007058634-A1; EP1948224-A1; ZA200803889-A, 2007.

[105] R. Rucman and P. Zupet, WO2008150245-A2; WO2008150245-A3; EP2164469-A2; CN101742986-A, 2009.

[106] D. Churchley and A. Amberkhane, WO2008050185-A2, 2008.

[107] S. N. Devarakonda, M. Asnani, S. R. Bonnareddy, P. R. Padi, U. K. Chandramohan, S. S. Chitre, V. Nalivella, S. K. Vasamsetti, A. Minakshi, B. S. Reddy, and P. P. Reddy, WO2007092758-A2; WO2007092758-A3; IN200804031-P4, 2008.

[108] R. Rucman and P. Zupet, EP1647547-A1, 2006.

[109] M. Piran, M. Cohen, S. Costi, M. Khan, M. Gharpure, A. K. Pandey, R. S. Yadav, P. V. Patil, S. Lad, and G. Patle, WO2010148396-A1, 2010.

[110] N. J. Brown and D. E. Vaughan, Angiotensin-converting enzyme inhibitors. *Circulation*, 97, (1998):1411.
[111] M. Remko, Acidity, lipophilicity, solubility, absorption, and polar surface area of some ACE inhibitors. *Chemical Papers*, 61, (2007):133.
[112] L. Fabian, Cambridge Structural Database Analysis of Molecular Complementarity in Co-crystals. *Crystal Growth & Design*, 9, (2009):1436.
[113] N. S. Joshi, S. B. Bhirud, and K. E. Rao, US2005250706-A1; WO2005108365-A1; IN200400531-I3; IN220637-B, 2005.
[114] V. Andre, L. Cunha-Silva, P. P. Santos, and M. T. Duarte, Portugal Patent, No., 2010.
[115] E. H. H. Chow, F. C. Strobridge, and T. Friscic, Mechanochemistry of magnesium oxide revisited: facile derivatisation of pharmaceuticals using coordination and supramolecular chemistry. *Chemical Communications*, 46, (2010):6368.
[116] T. Friscic, New opportunities for materials synthesis using mechanochemistry. *Journal of Materials Chemistry*, 20, (2010):7599.
[117] D. R. Weyna, T. Shattock, P. Vishweshwar, and M. J. Zaworotko, Synthesis and Structural Characterization of Co-crystals and Pharmaceutical Co-crystals: Mechanochemistry vs Slow Evaporation A from Solution. *Crystal Growth & Design*, 9, (2009):1106.
[118] A. V. Trask, D. A. Haynes, W. D. S. Motherwell, and W. Jones, Screening for crystalline salts via mechanochemistry. *Chemical Communications*, (2006):51.
[119] T. Friscic and W. Jones, Recent Advances in Understanding the Mechanism of Co-crystal Formation via Grinding. *Crystal Growth & Design*, 9, (2009):1621.

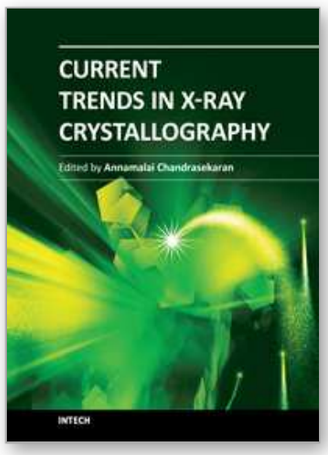

Current Trends in X-Ray Crystallography

Edited by Dr. Annamalai Chandrasekaran

ISBN 978-953-307-754-3
Hard cover, 436 pages
Publisher InTech
Published online 16, December, 2011
Published in print edition December, 2011

This book on X-ray Crystallography is a compilation of current trends in the use of X-ray crystallography and related structural determination methods in various fields. The methods covered here include single crystal small-molecule X-ray crystallography, macromolecular (protein) single crystal X-ray crystallography, and scattering and spectroscopic complimentary methods. The fields range from simple organic compounds, metal complexes to proteins, and also cover the meta-analyses of the database for weak interactions.

How to reference

In order to correctly reference this scholarly work, feel free to copy and paste the following:

Vânia André and M. Teresa Duarte (2011). Novel Challenges in Crystal Engineering: Polymorphs and New Crystal Forms of Active Pharmaceutical Ingredients, Current Trends in X-Ray Crystallography, Dr. Annamalai Chandrasekaran (Ed.), ISBN: 978-953-307-754-3, InTech, Available from: http://www.intechopen.com/books/current-trends-in-x-ray-crystallography/novel-challenges-in-crystal-engineering-polymorphs-and-new-crystal-forms-of-active-pharmaceutical-in

INTECH
open science | open minds

InTech Europe
University Campus STeP Ri
Slavka Krautzeka 83/A
51000 Rijeka, Croatia
Phone: +385 (51) 770 447
Fax: +385 (51) 686 166
www.intechopen.com

InTech China
Unit 405, Office Block, Hotel Equatorial Shanghai
No.65, Yan An Road (West), Shanghai, 200040, China
中国上海市延安西路65号上海国际贵都大饭店办公楼405单元
Phone: +86-21-62489820
Fax: +86-21-62489821

IntechOpen